Catalysis Science & Technology

Selective deoxygenation of polar polymers using metal supported on TiO_2 nanotubes

Journal:	*Catalysis Science & Technology*
Manuscript ID	CY-ART-03-2024-000404.R1
Article Type:	Paper
Date Submitted by the Author:	27-Jun-2024

Complete List of Authors:	Bui, Dai Phat; The University of Oklahoma, Sustainable Chemical, Biological and Materials Engineering Gomez, Laura; University of Oklahoma, Sustainable Chemical, Biological and Materials Engineering Alalq, Ismael; University of Oklahoma Trevisi, Luis; The University of Oklahoma, Chemical, Biological and Materials Engineering Jerdy, Ana Carolina; University of Oklahoma, Chemical, Biological and Materials Engineering Chau, Han; The University of Oklahoma, Chemical, Biological and Materials Engineering Lobban, Lance; University of Oklahoma Crossley, Steven; University of Oklahoma, Sustainable Chemical, Biological and Materials Engineering

Data Availability Statement:

The data supporting this article have been included as part of the Supplementary Information.

Selective deoxygenation of polar polymers using metal supported on TiO_2 nanotubes

Received 00th January 20xx,
Accepted 00th January 20xx

DOI: 10.1039/x0xx00000x

Dai-Phat Bui, Laura A. Gomez, Ismael Alalq, Luis Trevisi, Ana Carolina Jerdy, Han K. Chau, Lance L. Lobban, Steven P. Crossley*

Polar polymers such as poly(vinyl alcohol-co-ethylene) (EVOH) serve as excellent oxygen barriers in multilayered polymer films. However, their presence creates significant challenges for subsequent recycling. Melting and thermal degradation leave behind small domains of immiscible phases that render the final material less valuable. Here, we report a strategy to selectively remove OH groups from the EVOH polymer while preserving the polymer's hydrocarbon backbone. Pd supported on TiO_2 nanotubes exhibit excellent abilities in dehydration and hydrogenation. This is evidenced in our study, which utilizes both the model compound 2,5-hexanediol (a small surrogate for polyols) and EVOH. The Lewis-acid sites generated on the TiO_2 surface, coupled with hydrogen spillover from the metal particles, result in enhanced dehydration rates, while subsequent hydrogenation at atmospheric pressure generates saturated products. The intimacy between Pd particles and their TiO_2 supports for EVOH conversion is also discussed.

1. Introduction

The polymer industry produces more than 400 million metric tons of polymers annually and is projected to reach 700 million metric tons by 2030.[1] Less than 10% of the polymers are recycled, with the majority either incinerated or landfilled, which may create secondary pollutants that negatively affect the environment.[2] Several solutions are often implemented to recycle these discarded plastics.[3,4] Among these solutions, mechanical recycling has been implemented; however, this approach brings limitations when attempting to produce high-value products.[3,4] While chemical recycling and upcycling have proven effective for some well-known polymers, different chemical strategies are often needed to regenerate high-value monomers or valuable chemicals from some of the most common streams.[4–7] However, implementing these approaches becomes challenging if feedstock streams contain additives or multiple resins that cannot be separated through conventional physical sorting methods.[8,9]

As the industry evolved, multilayered films have gained greater importance, as these multiple thin films of different polymers can better fulfill consumer needs while minimizing material utilization.[10–12] However, this creates a dilemma. While the use of multilayered films leads to beneficial outcomes such as prolonged product shelf life and lower package weight, leading to decreased CO_2 emissions associated with transportation,[13] the primary drawback of these more advanced multicomponent films is that they are extremely challenging to recycle.

Multilayered films often contain barrier film layers, such as poly (vinyl alcohol-co-ethylene) (EVOH), which is widely used as an oxygen barrier for food and pharmaceutical packaging.[14] These films also involve tie layers that can become immiscible with the other layers upon melting. In some cases, the concentration of these polar polymers, such as EVOH, may be very low, making extraction difficult or economically challenging. If these low-abundance species could be selectively converted into more compatible components, some of these existing recycling strategies may be employed. While selective conversion of polyols to remove oxygen groups is in its early stages of exploration,[15,16] selective deoxygenation has been extensively studied with smaller biomass-derived species in recent years.[17,18]

We propose a new strategy for the catalytic conversion of EVOH to form compatible polymer streams, as shown in **Figure 1**. This strategy relies on catalytic deoxygenation through direct C-O bond scission or sequential dehydration to effectively remove oxygen, followed by hydrogenation. The goal is to improve compatibility with other polymers (typically polyolefins) while avoiding the cleavage of carbon-carbon bonds on the polymer backbone. This approach aims to maximize the amount of compatible polymer in the recycle stream and minimize waste. Our prior efforts with monofunctional acid catalysts have illustrated the potential for selective conversion of alcohol functional groups; however, this has not yet been coupled with metals to hydrogenate resulting products and ultimately yield a polymer that is chemically similar to polyethylene.[15,16]

Some metals supported on reducible oxides, such as Pd/TiO_2, exhibit the promise of enabling selective C-O bond scission reactions while avoiding excess C-C hydrogenolysis.[19–21] This family of catalysts is known to create highly active sites at the metal-support interface.[22] The addition of Pd metal clusters, which can be reduced at modest temperatures compared to most other noble metals, typically promotes hydrogen dissociation, leading to hydrogen spillover across the surface. Consequently, this process can modulate the number of exposed cations by removing lattice O groups and increasing the number of exposed sites capable of dehydration reactions.[23] Hydrogen spillover also modifies the density of OH groups at the surface, which is known to modify the interaction of molecules with the catalyst surface.[24] This could have significant implications in polymer conversion, given the importance of polymer-support interactions in modifying product distributions.

[a] *School of Sustainable Chemical, Biological and Materials Engineering, University of Oklahoma, Norman, OK 73019, United States. Email: stevencrossley@ou.edu*
Electronic Supplementary Information (ESI) available: [details of any supplementary information available should be included here]. See DOI: 10.1039/x0xx00000x

It is well known that most polymers are readily prone to diffusion limitations on most traditional microporous catalysts.[25,26] Here, TiO_2 nanotubes were synthesized to mitigate these limitations since the external surface of nanotubes is effectively an inverted pore structure, offering high amounts of accessible surface area on the external of the nanotubes without internal diffusion restrictions accompanying most high surface area catalysts.[27] A shorter diffusion path, as we envision, would occur when reactions take place directly on the external surface of a tube, would lead to a minimization of secondary reactions along the diffusion path in a solid, highly microporous catalyst, which are often misunderstood as intrinsic attributes of the active site.[28-30] To improve the redox properties of TiO_2 at lower temperatures, the reducible support was functionalized with Pd metal clusters. Thus, the incorporation of Pd clusters can enhance dehydration/hydrogenation rates by the hydrogenation of products and modification of the catalytic activity of the TiO_2.[30] This study is intended to advance understanding of the catalytic features necessary to selectively convert polar hydroxyl groups in multicomponent films such that the barriers to recycle these materials are reduced.

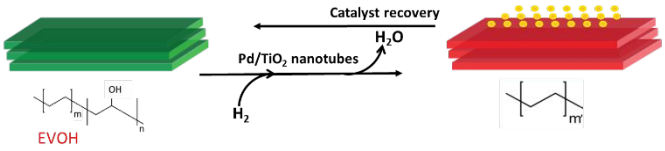

Figure 1. Strategy for catalytic conversion of EVOH over a reducible metal support.

2. Experimental

2.1 Chemicals

2,5-dimethyltetrahydrofuran (DMTHF, 96%), 2,5-hexanediol (99%), 2-hexanol (99%), γ-valerolactone (GVL, 99%), poly(vinyl alcohol-co-ethylene) (EVOH, T_m = 180 °C, 32 mol % ethylene), SiO_2 (nanopowder, 10-20 nm particle size), tetradecane (99%), $Pd(NO_3)_2.2H_2O$ (~40% Pd basis), and TiO_2 (nanopowder < 25 nm, mixture of rutile: anatase/85:15) were purchased from Sigma Aldrich. Deuterated dimethyl sulfoxide-d6 (DMSO, 99.9%) was purchased on MagniSolv. Single-wall carbon nanotubes (CNTs) were purchased from SweNT. The gases were obtained from Airgas: Nitrogen (N_2, ultra-high purity GD 5.0) and hydrogen (H_2, ultra-high purity GR 5.0 CGA 350). A gas mixture of 5% CO/He and 5% O_2/He was used for CO and O_2 chemisorption, respectively.

2.2 Polymer preparation

The polymer used in this study, EVOH, was pulverized using a Retsch Mixer Mix CryoMill with a 50 mL grinding jar, one 25 mm grinding ball with a profile of 10 minutes of pre-cooling at 5 Hz, followed by three cycles of grinding for 10 minutes at 25 Hz, with an intermediate cooling step of 5 minutes at 5 Hz. NMR results, presented in Table S1, indicate that the functional groups in pellet EVOH (in its purchased state) remain unchanged compared to EVOH after the cryomilling step. This polymer pretreatment was conducted to facilitate initial mixing and enhance catalyst contact for TGA studies. For the other experiments using a semi-batch reactor, EVOH was used in pellet form. NMR analysis was conducted before and after to validate that the polymer did not undergo mechanical decomposition during the cryomilling pretreatment, revealing no significant differences, as indicated in **Table S1**.

2.3 Catalyst Preparation

To synthesize TiO_2 nanotubes (TNTs), 1.7 g of TiO_2 was dispersed in 157 mL of NaOH 10 M solution before undergoing the hydrothermal process at 135 °C for 24 h. The resulting hydrothermal mixture was neutralized with HCl, washed multiple times with DI water, and subsequently dried at 60°C.[31]The resulting powder then calcinated at 350 °C for 2 h.

The incipient wetness impregnation method was employed to synthesize 2 wt % Pd over TiO_2 nanotubes (Pd/TNTs), utilizing $Pd(NO_3)_2.2H_2O$ as a Pd precursor. A similar approach was conducted for all the supports investigated in this study (SiO_2, TiO_2, and CNT). After synthesis, all the catalysts were dried at 80 °C for 12 h in a vacuum oven before undergoing a calcination process at 350 °C for 2 h.

2.4 Characterization

The morphology and distribution of the catalysts were monitored by a Field Emission Gun Transmission Electron Microscope (FEG-TEM) and energy-dispersive X-ray spectroscope (EDX), respectively. The TEM images were recorded using a JEOL JEM 2010F in an ultra-high vacuum. The catalyst powder was dispersed in DI water and coated on a copper mesh before placing it in the vacuum chamber. The surface area and pore volume of the catalysts were measured using a Micromeritics ASAP 2010 instrument. The mass loss and product formation of the dehydration and hydrogenation of EVOH over the catalysts were monitored by a Netzsch STA F1 thermogravimetric analysis (TGA) system coupled with a QMS Aeolos 403C mass spectrometer.

2.5 Chemisorption Experiments

Oxygen chemisorption experiments were conducted to quantify the number of oxygen vacancies created under reaction conditions. For this experiment, 50 mg of catalyst mass were mixed with glass beads (150 mg) and reduced for 30 minutes at 190°C to promote oxygen vacancy formation, followed by inert gas treatment at room temperature to remove hydrogen atoms that could present at the catalyst surface. Small doses of O_2 were then introduced through the catalyst bed using a micro-pulse reactor at 350°C. A similar setup was used for the CO chemisorption, which was employed to quantify the exposed Pd metal sites. The Pd/TNTs were reduced at 100°C previous to the CO chemisorption to avoid further reduction of the support. Subsequently, CO pulses were introduced at room temperature.

2.6 Catalytic reactions

A gas phase dehydration reaction of 2,5-hexanediol over different catalyst samples (TNTs, Pd/TNTs, Pd/TiO_2, TiO_2) was carried out in a fixed bed tubular reactor. A measured amount of pelletized (250-355 µm) catalyst of 20 mg mixed with glass beads packed between quartz wools in a 1/4-inch quartz reactor tube was then pretreated at 10°C/min to 200°C under flowing hydrogen and held for 30 minutes to stabilize reactor for reaction temperatures at 200°C. The hydrogen carrier gas was set at 100 ml/ min, and the feed was introduced in a mixture of 2,5-hexanediol and GVL (1:5 volume ratio) with flow rates between 0.4-0.6 mL/h, which was controlled using syringe pumps. The reactor temperature was controlled via an attached thermocouple to the external surface of the reactor tube aligned with the center of the catalyst bed. The reactor outlet streamline was heated to 300°C to avoid condensation of leaving species. A micro electric actuator controlled the six-port valve used to send the sample to an inline connected gas chromatograph HP 6890 GC-FID equipped with a flame ionization detector and an Agilent HP-INNOWAX (L × ID × thickness = 30m ×0.32mm ×0.50µm) column for separation of molecules in this reaction. The rates were extrapolated to zero time on stream to rule out the deactivation effect on the overall rate.

The response factor was achieved by flowing the reactant at the desired rate through a glass beads bed to mimic the catalyst bed. These response factors are used for further data analysis, such as conversion and carbon balance. The reaction rates were obtained using Eqn. (1):

$$reation\ rate\ (r) = \frac{Moles\ of\ product\ formed}{time\ *\ mass\ of\ catalyst}\ (\frac{mol}{hour\ gram}) \quad (1)$$

The product formation yields of each species were estimated by using Eqn. (2):

$$Yield = \frac{Moles\ of\ a\ product\ formed\ per\ hour}{Moles\ of\ 2{,}5-hexanediol\ fed\ per\ hour}\ (mol\%) \quad (2)$$

The dehydration and hydrogenation of EVOH were conducted in a thermogravimetric analyzer (TGA) and semi-batch reactor at 195 °C in H_2. In the TGA setup, the EVOH powder and 10 wt % of the catalyst were mixed at room temperature using a vortex system to ensure thorough mixing and effective contact with the catalyst. The mixtures were transferred into crucibles in the TGA to conduct the reactions, using the temperature profiles as follows: Segment 1, the temperature was raised from 30 °C to 150 °C at a ramping rate of 10 K/min to desorb the adsorbed H_2O on the surface of both EVOH and the catalyst. Segment 2 was held at 150 °C for 30 min to pretreat the catalyst under H_2 gas. Subsequently, in segment 3, the temperature was increased from 150 °C to 195 °C at a ramping rate of 5K/min. Lastly, in segment 4, the temperature was held at 195 °C for 1 h to carry out the dehydration and hydrogenation of EVOH.

For EVOH reactions in a semi-batch reactor, the reaction was conducted in a 50 mL three-neck round bottom flask 14/20 with one neck connected to the gas line, another connected to a condenser, and the third neck was used for chemical injection. Initially, 10 mg of catalyst and 2 mL of GVL were combined at room temperature under N_2, followed by the continuous introduction of H_2. The mixture was heated to 150 °C for 30 min to treat the catalyst before adding 100 mg of EVOH pellets. Afterward, the mixture was heated to 195 °C and held at this temperature for 1 h to achieve the dehydration and hydrogenation of the EVOH. The EVOH and catalyst were then removed from the GVL mixture via cooling. Here, GVL was chosen as the green solvent for the reaction of EVOH and 2,5-hexanediol because it is a stable polar solvent and can be readily derived from biomass.

The components of EVOH before and after the reaction over the catalysts were characterized by Proton nuclear magnetic resonance (proton NMR). The polymer-sample mixture was introduced to the DMSO NMR solvent at 80 °C, after which the polymer mixture was fully dissolved. All reaction products were also fully dissolved in DMSO after the reaction, with no observed precipitation of polymer products in the NMR solvent. The proton NMR signals were recorded using a Varian VNMRS 400 MHz NMR Spectrometer. Prior to these experiments, an inverse recovery pulse sequence was employed to acquire the maximum spin-lattice relaxation (T1) for both the solvent (DMSO-d6) and the polymers (EVOH and reacted EVOH). This was done to ensure that the relaxation time could be set at five times the value of T1 for accurate and quantitative measurements. In this specific sample and environment, the longest T1 observed was 0.9 s. As a result, the relaxation delay utilized for all measurements was fixed at 5s. The spectral width was set at 6410.3 Hz, the acquisition time was 2.556 s, complex points were set to 16384, the pulse angle was set at 90 degrees, and a total of 128 scans were conducted.

3. Results and discussion

3.1 Catalyst Characterization

Figure 2a illustrates the results of TEM analysis conducted on both TNTs and Pd/TNTs. The TNT catalyst exhibits an average inner diameter and length of about 7.1 nm and 125 nm, as shown in **Figure 2b**. The presence of Pd metal clusters was verified using Energy Dispersive X-ray (EDX) mapping of Pd/TNTs, as illustrated in **Figure 2c**. SEM and EDX analysis shows similar results, **Figure S1**. The physical characteristics of the TiO_2 catalysts measured by N_2 adsorption are provided in **Table 1**. As a result, the surface area of TNTs (156.2 m^2/g) is around 3.5 times higher than that of TiO_2 (44.1 m^2/g). Thus, the unique nanotube structure can further facilitate the accessibility of a significant portion of this surface area to large polymer molecules. The surface area and pore volume of the Pd-supported catalyst were also measured, as shown in **Table S2**. It is important to note that while other inert supports may have high surface areas, they lack the unique sites present in TNTs that are crucial for selective deoxygenation chemistry, which Pd alone cannot achieve.

Table 1. Surface area and pore volume of TiO_2 catalysts

Catalyst	Surface area (m^2/g)	Pore Volume (cm^3/g)	Micropore Volume (cm^3/g)
TiO_2	44.1	0.25	0.0012
TNTs	156.2	0.72	0.0114

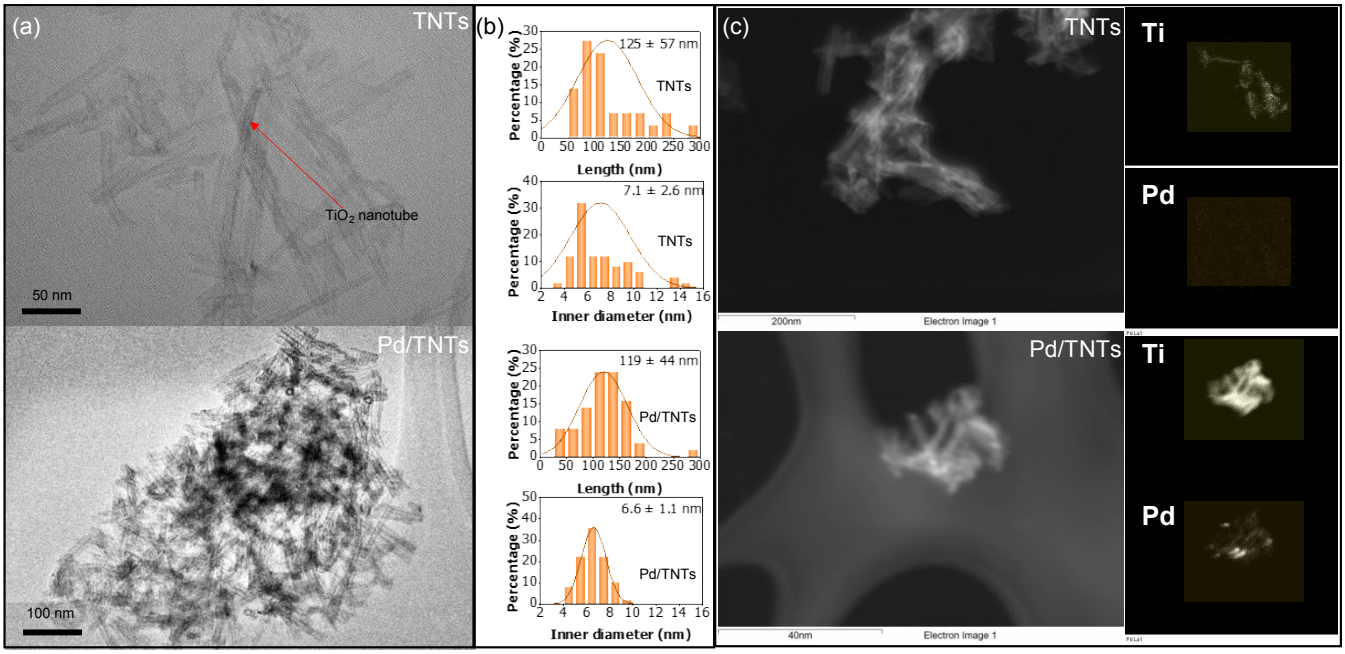

Figure 2 (a) TEM images of TNTs and Pd/TNTs, (b) Size distribution of inner diameter and length tube for TNTs and Pd/TNTs, and (c) EDX mapping of TNTs and Pd/TNTs.

Oxygen chemisorption was utilized as a probe molecule technique to quantify the number of oxygen vacancies formed under H_2 reduction conditions. Several studies indicate that surface defects on TiO_2 favor O_2 dissociation, which leads to the titration of two oxygen vacancies, even at low temperatures.[32,33] **Figure 3a** indicates that the incorporation of Pd metal clusters drastically increases the number of oxygen vacancies at the surface, which explains the high dehydration rate yield for Pd/TNTs. The amount of oxygen uptake over Pd catalysts was corrected by also carrying out O_2 chemisorption experiments over a Pd/SiO_2 catalyst and subtracting this amount of oxygen uptake per Pd atom from the Pd/TiO_2 and Pd/TNTs catalysts.

Table 2. Results of CO chemisorption studies. Values of dispersion, mean diameter, and specific surface area for Pd/TiO_2 and Pd/TNTs.

	Pd/TiO_2	Pd/TNTs
D (%)	73.7	82.5
d_{VA} (nm)	1.5	1.3
S_{sp} ($m^2\ g^{-1}$)	332.24	371.65
Ns	5.0×10^{18}	5.6×10^{18}
Nt	6.8×10^{18}	6.8×10^{18}

D: Dispersion; $\mathbf{d_{VA}}$: Diameter; S_{sp}: Specific surface area; N_s: Total number of Pd metal atoms on the surface; N_t: Total number of Pd metal atoms (surface and bulk).

Utilizing CO titration, we determined the size of Pd particles and the proportion of exposed Pd atoms, as shown in **Table 2**. A stoichiometric ratio of 2 for Pd/CO chemisorption was considered to quantify the exposed metals. This assumption is based on the premise that CO-adsorbed molecules form a bridge bond with Pd atoms.[34] Pd/TiO_2 and Pd/TNTs exhibited a similar mean Pd particle size, with respective values of 1.5 nm and 1.3 nm.

3.2 Conversion of 2,5-Hexanediol over Pd supported TiO_2 nanotubes

To gain initial insights into the capability of reducible oxide catalysts in promoting EVOH deoxygenation, we utilized 2,5-hexanediol as a model compound. 2,5-hexanediol and its isomers have been used previously as a surrogate to understand the catalytic conversion of EVOH under conditions not corrupted by diffusion limitations.[15,16] GVL was chosen as the green solvent for the reaction of EVOH and 2,5-hexanediol because it is a stable polar solvent and can be readily derived from biomass.[35,36] This model compound was tested by using different catalyst supports: SiO_2 (inert support), Pd/SiO_2 (metallic sites), Pd/CNTs (metal site on non-acid site with high surface area support), TiO_2 powder, TiO_2 nanotubes (TNTs), Pd/TiO_2, Pd/TNTs, and a physical mixture of Pd/CNTs and TNTs.

Figure 3b illustrates the conversion of 2,5-hexanediol across different catalysts: TiO_2, TNTs, Pd/TiO_2, and Pd/TNTs, resulting in conversion rates of 45.4%, 60.2%, 62.2%, and 67.4%, respectively. Notably, all tested catalysts exhibit a selectivity equal to or exceeding 90% towards the primary product, 2,5-dimethyl tetrahydrofuran (DMTHF). Furthermore, as a secondary product, 2-hexanol is observed only over Pd/TiO_2 and Pd/TNTs catalysts, where DMTHF undergoes an additional hydrogenation reaction, leading to the formation of saturated 2-hexanol. Thus, the abundance of DMTHF in the product distribution illustrates that the initial dehydration step is fast, followed by a slow decomposition of the ether bond under these conditions, which is aligned with observations from prior studies.[15] Comparable experiments were performed using inert support catalysts such as SiO_2, Pd/SiO_2, and Pd/CNTs. These trials demonstrated minimal conversion of 2,5-hexanediol into DMTHF or 2-hexanol. In contrast, Pd/CNTs + TNTs exhibited notable activity, primarily attributed to the Lewis acids sites located on the TNTs. These findings align with prior reports suggesting that the interface between metals and reducible

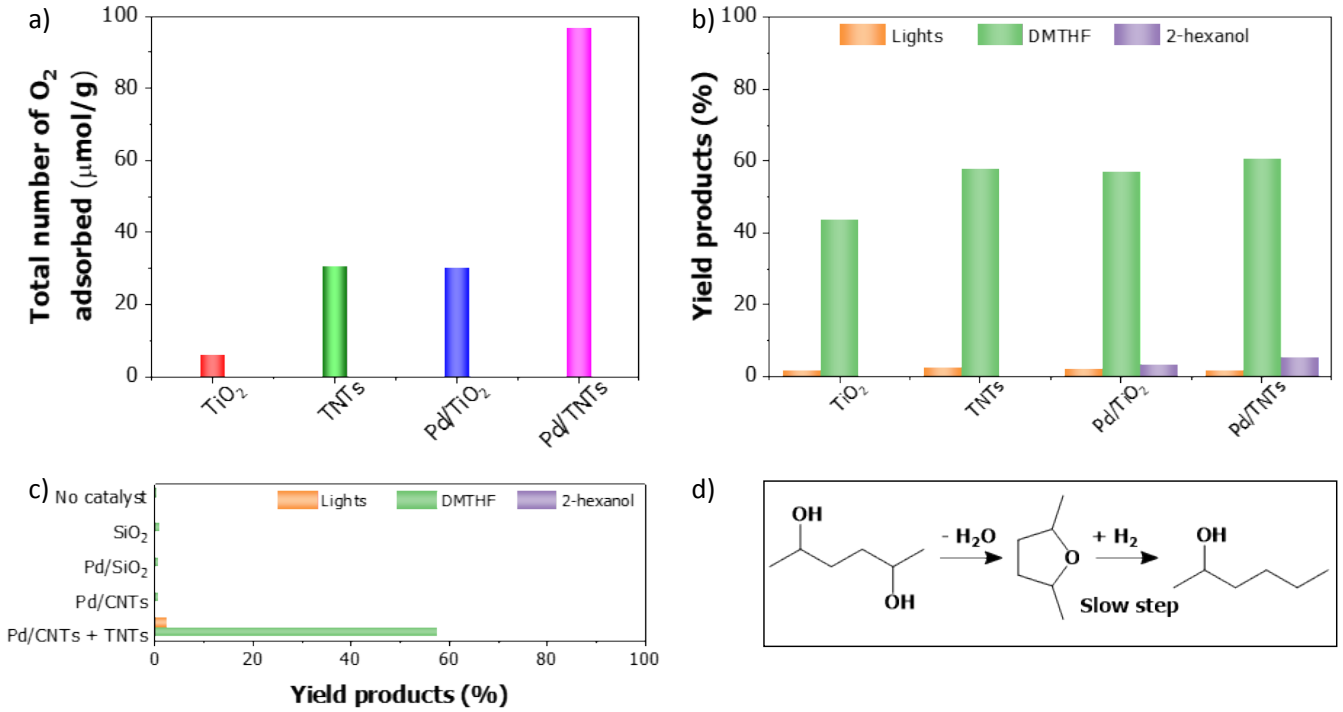

Figure 3 (a) O_2 chemisorption results for TiO_2, TNTs, Pd/TiO_2, and Pd/TNTs. Reaction conditions: $T_{reduction}$ = 190°C, $T_{chemisorption}$ = 350°C, and $W_{cat.}$ = 50 mg. (b) Yields of 2,5-hexanediol dehydration and hydrogenation over TiO_2, TNTs, Pd/ TiO_2, and Pd/TNTs in a gas phase reactor. (c) Yields of 2,5-hexanediol dehydration and hydrogenation over SiO_2, Pd/SiO_2, Pd/CNTs, and Pd/CNTs + TNTs and without catalyst in a gas phase reactor. Reaction conditions for (b) and (c) are the same: $T_{reaction}$ = 200°C, $W_{cat.}$ = 20 mg, F_{H2} = 100 ml/ min, F_{Feed}= 0.6 mL/h. For all the cases, the feed was introduced in a mixture of 2,5-hexanediol and GVL (1:5 volume ratio). For the physical mixture of Pd/CNT + TNTs, 20mg of Pd/CNT and 20mg TNTs were used. (d) Proposed reaction pathway.

supports can facilitate the hydrogenation and hydrogenolysis of C-O and C-O-C.[37–39] Pd/CNTs further enhanced the activity towards lighter compounds, as illustrated in **Figure 3c**.

The incorporation of Pd metal clusters directly over a reducible metal oxide introduces two additional important features. Firstly, interfacial sites at the metal/support interface are well known for their high activity in activating C-O bonds.[21,22] These interfacial sites at the perimeter of the metal and TiO2 support have been shown to lead to activate said bonds due to strong O interaction with undercoordinated sites on the Ti while the connecting C is bound to the noble metal, thus enhancing C-O cleavage rates. Secondly, the presence of Pd metal clusters promotes hydrogen spillover from the metal sites to the reducible oxide support. This modifies the formation of surface OH groups and oxygen vacancies, tunning the catalytic activity of the TiO_2 surface. These undercoordinated centers could also serve to dehydrate alcohols to yield olefins, which could then migrate to the metal to undergo hydrogenation. Kinetic deconvolution of these phenomena is challenging and should be a point of future studies.[19,21,40] To test the importance of sites located at the interface of Pd/TNTs, a physical mixture of TNTs and Pd/CNTs was used. **Figure 3c** indicates that the absence of direct contact of Pd and TNTs does not result in the formation of 2-hexanol, nor does it lead to a substantial increase in the yield of DMTHF. However, small yields for light products were observed for this physical mixture (Pd/CNTs + TNTs), resulting from consecutive dehydration and hydrogenation reactions of the products. Hence, these findings suggest that the ring-opening chemistry of DMTHF to hexanol is likely to be predominantly facilitated at the interface sites of Pd/TiO_2. Gilkey et al. demonstrated that the conversion of 2,5-dimethylfuran (DMF) via ring-opening to 2-hexanol and 2-hexanone through ring-opening chemistry is unlikely to take place on monometallic surfaces but rather occurs in bi- or multifunctional catalysts.[41] Our group has similarly shown that over metal supported on TiO_2 surfaces, for cresol conversion,[21] furfuraldehyde deoxygenation,[19] and furan ring opening and rearrangement,[22] the kinetically relevant active site for this selective chemistry lies at the metal/support interface.

The reaction pathway can be hypothesized, as illustrated in **Figure 3d**, involving the dehydration of 2,5-hexanediol to form a cyclic ether before undergoing hydrogenation, which furthermore can undergo ring opening to yield 2-hexanol.

3.3 EVOH conversion over Pd-supported TiO_2 nanotubes

The dehydration and hydrogenation of EVOH were also investigated via thermal gravimetric analysis (TGA) at 195°C under a reducing environment. As shown in **Figure 4a**, EVOH is thermally stable under reaction conditions in the absence of a catalyst. As a result, the addition of 2 mg TiO_2 or 2 mg TNTs to 20 mg EVOH results in 0.3% and 1% mass loss, corresponding to approximately 1% and 3.4% of the total hydroxyl groups in EVOH, respectively. The mass spectra further confirmed that the weight lost under these conditions is only attributed to EVOH dehydration, leading to the generation of water as a byproduct, as is shown in **Figure S2**. Upon incorporation of Pd metal clusters over TNTs, the mass loss significantly increases to 5.7%. This indicates the removal of 18.7 % of the total hydroxyl groups present in EVOH, as shown in **Figure 4b**. Therefore, the

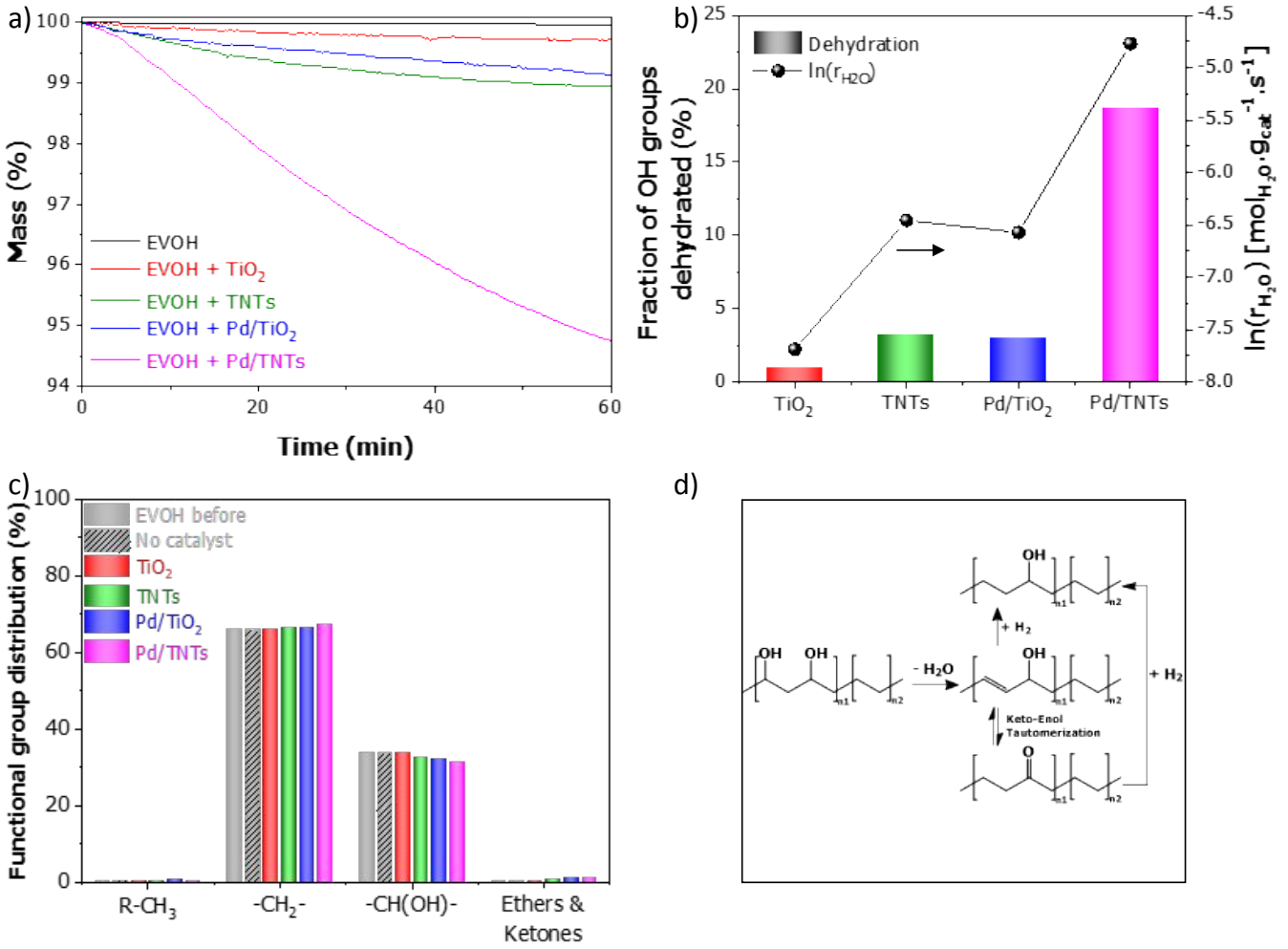

Figure 4 (a) TGA results of dehydration and hydrogenation of EVOH over TiO_2, TNTs, Pd/TiO_2, and Pd/TNTs catalysts. (b) Fraction of OH groups dehydrated (%) and rate of EVOH by using TiO_2, TNTs, Pd/TiO_2, and Pd/TNTs as a catalyst. (c) Functional group distribution of EVOH after reaction. (d) Polymer dehydrated/hydrogenated reaction products. Reaction conditions: $W_{cat.}$ = 2 mg, W_{EVOH}= 20 mg, F_{H2} = 40 mL/min and $T_{reaction}$= 195°C. The quantities for the functional groups related to ether and ketones were added together.

incorporation of Pd on TiO_2 or TNTs drastically increases the rates of dehydration. Similar studies were conducted using inert support catalysts such as SiO_2 and CNT, revealing that the absence of Lewis acid sites notably reduces the dehydration reaction of EVOH (**Figure S3**).

To further investigate the ability of the catalysts to selectively break C-O bonds, NMR analysis of the products can be seen in **Figure 4c** and **Figure S4**. The number of each species was determined by considering the number of hydrogen atoms per functional group: R-C*H*$_3$/3, R-C*H*$_2$-R/2, R-O*H*/1, RC*H*OR (link to ether or alcohols)/1, and ketones/4. The residual oxygen species were assessed by measuring the combined H signal from the region corresponding to RCHOR (3.5-4.2 ppm) and Ketones (2-2.5 ppm). The number of ketones was measured by leveraging the distinctive shift in the adjacent CH_2 groups caused by this functionality (1.8-2.3 ppm). The stoichiometric number of protons associated with CH_2 groups was determined by adding the summing of the primary peak of both unaffected CH_2 groups (1-1.7 ppm) and the CH_2 groups that experienced a shift due to ketone functionality (1.8-2.3 ppm). Subsequently, the quantity of ether groups was estimated by subtracting the R-OH (4.2-4.7 ppm) from the RCHOR groups. A summary of the chemical shift ranges for the functional groups involved in the deoxygenation of EVOH is indicated in **Table S3**.

The dehydration of EVOH over TiO_2 and TNTs increases with the amount of residual oxygens species representing the ketones and ethers in the polymer chains, as indicated in **Figure 4c**. EVOH dehydration over Pd/TNTs is followed by hydrogenation, which significantly increases the -CH_2-CH_2- products representative of the conversion of polyvinyl alcohol (PVA) to PE-like polymers in the final products (**Figure S4**). The persistent presence of residual oxygen products indicates that further hydrogenation activity through either more metal functionality or increased hydrogen pressures would further increase rates of PE-like products. From these results, the dehydration and hydrogenation of EVOH over Pd/TNTs are assumed to occur through initial dehydration over the TNT surface, after which the dehydrated products may undergo two routes. Unsaturated products may be hydrogenated via the metal function, while the residual acid sites may facilitate

ketone formation via double bond migration and keto-enol tautomerization (**Figure 4d**).[42] Thusgiven sufficient reaction time, these residual oxygen species may be further converted to saturated products over the metal function. Alternatively, if highly active sites for C-O cleavage at the metal-support interface play an important role, the direct production of saturated products will lead to lower yields of olefinic and ketone products.

To further study the dehydration and hydrogenation of EVOH, a semi-batch stirred reactor on a larger scale was used to improve external diffusion to the catalyst particles. The polymer reaction products were analyzed by NMR (**Figure 5a**). Because GVL was used as a solvent, the residual overlapping GVL signals were subtracted from the -CH_2- contribution (**Figure S5**).

EVOH conversion in a semi-batch reactor yields a similar trend in reaction products, aligning with the findings obtained

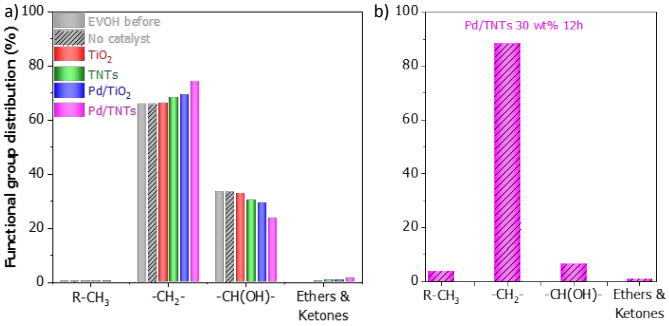

Figure 5. Functional group distribution (%) of EVOH after reaction in a semi-batch reactor (a) after 1 h of reaction over TiO_2, TNTs, Pd/TiO_2, and Pd/TNTs. (b) After 12 h of reaction over Pd/TNTs. Reaction conditions: (a) $W_{cat.}$ = 10 mg or (b) $W_{cat.}$ = 30 mg; F_{H2}= 60 mL/min, W_{EVOH}= 100 mg, $T_{reaction}$= 195°C. For all the cases, 2 mL of GVL was used as a solvent. The quantities for the functional groups related to ether and ketones were added together.

with TGA analysis. TiO_2 and TNTs can dehydrate much more in a well-mixed system, decreasing PVA content in the final products. However, the content of PE is similar for both catalysts, attributable to insufficient hydrogenation. **Figure 5a** indicates that Pd/TNTs exhibit the highest yields for both dehydration and hydrogenation rates. Using Pd/TNTs as catalysts, OH groups in polymer chains significantly decreased from 33.6% to 23.7%, while the -CH_2- portion increased from 65.9% to 74.4%. Thus, less residual oxygen products are observed compared to reactions conducted in TGA crucibles.

Similar studies were conducted on inert support catalysts such as SiO_2, Pd/SiO_2, and Pd/CNTs. However, as shown in **Figure S6**, the results indicated that dehydration/hydrogenation of EVOH does not occur on monometallic surfaces. In contrast, a physical mixture of Pd/CNTs and TNTs shows a slight increase in the dehydration/hydrogenation rates. This implies that most of the dehydration/hydrogenation of EVOH occurs when Pd and TiO_2 or TNTs are in direct contact at sites located at the Pt/support interface as has been reported in many other deoxygenation reactions,[19,22] or that dehydrated polymers diffuse along the same particle to undergo hydrogenation prior to equilibrating with the solvent phase. These results align with results observed by using 2,5-hexanediol.

The conversion can be extended to achieve higher dehydration rates by increasing the reaction time or catalyst loading. **Figure 5b** shows the reduction of the vast majority of residual OH groups with only a minor increase in the number of CH_3 groups after 12 h. These results were compared with a blank reaction at 195°C for 12 hours using the most active catalyst (10mg of Pd/TNT), revealing no quantifiable losses in GVL solvent, as depicted in **Figure S7**. Additionally, NMR analysis of the products confirms the absence of any new peaks under these reaction conditions. Thus, this highlights the potential of this approach to convert polar functional groups while preserving the integrity of the hydrocarbon backbone.

4. Conclusions

This work shows the promise of Pd supported on TiO_2 nanotube (Pd/TNTs) catalysts for selective oxygen removal of polyols for both the model compound of 2,5-hexanediol as well as real EVOH streams, which is a common component of multilayered films. Our findings demonstrate that the incorporation of Pd metal clusters over TiO_2 nanotubes favors hydrogen spillover in combination with an increase of Lewis acid sites, significantly enhancing dehydration/hydrogenation rates while avoiding cleavage of the polymer backbone. It is revealed that 18.5% of OH groups of EVOH are dehydrated over Pd/TNTs, which outperforms other tested catalysts (Pd/TiO_2, Pd/SiO_2, Pd/C, and Pd/C+ TNTs). This conversion of PVA portions of EVOH to PE-like polymers could be highly promising for improved recycling of multicomponent polymer mixtures that cannot be physically sorted.

Author Contributions

D.-P.B.: Conceptualization, Investigation, Methodology, Validation, Visualization, Writing – Original Draft. LAG: Methodology, Investigation, Writing – Review & Editing. IA, LT, and ACJ: Methodology, Validation, Writing – Review & Editing. HKC: Methodology, Writing – Review & Editing. LLL: Conceptualization, Supervision, Project administration, Writing – Review & Editing. SPC: Conceptualization, Supervision, Project administration, Funding acquisition, Writing – Review & Editing.

Conflicts of interest

There are no conflicts to declare.

Acknowledgments

The authors are grateful for the financial support from the National Science Foundation under Grant No. EFRI E3P-2029394 to carry out this research. The authors acknowledge the support from the University of Oklahoma and thank Bin Wang, Kathy Wang, Jenna Holt, and Adam Feltz for the insightful discussions regarding the results.

References

1. Britt, P. F., Coates, G. W. & Winey, K. I. *Report of the Basic Energy Sciences Roundtable on Chemical Upcycling of Polymers*. *U.S. Department of Energy Office of Science* (2020).

2. Celik, G. *et al.* Upcycling Single-Use Polyethylene into High-Quality Liquid Products. *ACS Cent Sci* **5**, (2019).

3. Schyns, Z. O. G. & Shaver, M. P. Mechanical Recycling of Packaging Plastics: A Review. *Macromolecular Rapid Communications* vol. 42 Preprint at https://doi.org/10.1002/marc.202000415 (2021).

4. Tennakoon, A. *et al.* Catalytic upcycling of high-density polyethylene via a processive mechanism. *Nat Catal* **3**, (2020).

5. Liu, S., Kots, P. A., Vance, B. C., Danielson, A. & Vlachos, D. G. Plastic waste to fuels by hydrocracking at mild conditions. *Sci Adv* **7**, 8283–8304 (2021).

6. Vollmer, I. *et al.* Beyond Mechanical Recycling: Giving New Life to Plastic Waste. *Angew Chem Int Ed Engl* **59**, 15402–15423 (2020).

7. Kosloski-Oh, S. C., Wood, Z. A., Manjarrez, Y., De Los Rios, J. P. & Fieser, M. E. Catalytic methods for chemical recycling or upcycling of commercial polymers. *Mater Horiz* **8**, 1084–1129 (2021).

8. Zheng, J., Arifuzzaman, M., Tang, X., Chen, X. C. & Saito, T. Recent development of end-of-life strategies for plastic in industry and academia: bridging their gap for future deployment. *Materials Horizons* vol. 10 Preprint at https://doi.org/10.1039/d2mh01549h (2023).

9. Jerdy, A. C. *et al.* Impact of the presence of common polymer additives in thermal and catalytic polyethylene decomposition. *Appl Catal B* **325**, (2023).

10. Walsh, D. J., Su, E. & Guironnet, D. Catalytic synthesis of functionalized (polar and non-polar) polyolefin block copolymers. *Chem Sci* **9**, 4703–4707 (2018).

11. Wagner, J. R. *Multilayer Flexible Packaging: Second Edition*. *Multilayer Flexible Packaging: Second Edition* (2016). doi:10.1016/C2014-0-02918-8.

12. Walker, T. W. *et al.* Recycling of multilayer plastic packaging materials by solvent-targeted recovery and precipitation. *Sci Adv* **6**, (2020).

13. Pauer, E., Tacker, M., Gabriel, V. & Krauter, V. Sustainability of flexible multilayer packaging: Environmental impacts and recyclability of packaging for bacon in block. *Cleaner Environmental Systems* **1**, (2020).

14. Muriel-Galet, V., López-Carballo, G., Gavara, R. & Hernández-Muñoz, P. Antimicrobial Properties of Ethylene Vinyl Alcohol/Epsilon-Polylysine Films and Their Application in Surimi Preservation. *Food Bioproc Tech* **7**, (2014).

15. Chau, H. K. *et al.* Role of Water on Zeolite-Catalyzed Dehydration of Polyalcohols and EVOH Polymer. *ACS Catal* **13**, (2023).

16. Nguyen, Q. P., Chau, H. K., Lobban, L., Crossley, S. & Wang, B. Mechanistic insights into the conversion of polyalcohols over Brønsted acid sites. *Catal Sci Technol* (2023) doi:10.1039/d3cy00524k.

17. Omotoso, T., Boonyasuwat, S. & Crossley, S. P. Understanding the role of TiO2 crystal structure on the enhanced activity and stability of Ru/TiO2 catalysts for the conversion of lignin-derived oxygenates. *Green Chemistry* **16**, 645–652 (2014).

18. Boonyasuwat, S., Omotoso, T., Resasco, D. E. & Crossley, S. P. Conversion of guaiacol over supported Ru catalysts. *Catal Letters* **143**, (2013).

19. Briggs, N. M. *et al.* Identification of active sites on supported metal catalysts with carbon nanotube hydrogen highways. *Nat Commun* **9**, 3827 (2018).

20. Ellis, L. D., Ballesteros-Soberanas, J., Schwartz, D. K. & Medlin, J. W. Effects of metal oxide surface doping with phosphonic acid monolayers on alcohol dehydration activity and selectivity. *Appl Catal A Gen* **571**, (2019).

21. Omotoso, T. O., Baek, B., Grabow, L. C. & Crossley, S. P. Experimental and First-Principles Evidence for Interfacial Activity of Ru/TiO2 for the Direct Conversion of m-Cresol to Toluene. *ChemCatChem* **9**, 2642–2651 (2017).

22. Omotoso, T. *et al.* Stabilization of furanics to cyclic ketone building blocks in the vapor phase. *Appl Catal B* **254**, (2019).

23. Prins, R. Hydrogen spillover. Facts and fiction. *Chem Rev* **112**, 2714–2738 (2012).

24. Gomez, L. A. *et al.* Selective Reduction of Carboxylic Acids to Aldehydes with Promoted MoO3 Catalysts. *ACS Catal* **12**, 6313–6324 (2022).

25. Vollmer, I., Jenks, M. J. F., Mayorga González, R., Meirer, F. & Weckhuysen, B. M. Plastic Waste Conversion over a Refinery Waste Catalyst. *Angew Chem Int Ed Engl* **60**, 16101–16108 (2021).

26. Jerdy, A. C. *et al.* Deconvoluting the roles of polyolefin branching and unsaturation on depolymerization reactions over acid catalysts. *Appl Catal B* **337**, (2023).

27. Crossley, S., Faria, J., Shen, M. & Resasco, D. E. Solid nanoparticles that catalyze biofuel upgrade reactions at the water/oil interface. *Science* **327**, 68–72 (2010).

28. Crossley, S. P., Resasco, D. E. & Haller, G. L. Clarifying the multiple roles of confinement in zeolites: From stabilization of transition states to modification of internal diffusion rates. *J Catal* **372**, 382–387 (2019).

29. Gorte, R. J. & Crossley, S. P. A perspective on catalysis in solid acids. *J Catal* **375**, 524–530 (2019).

30. Hengsawad, T., Jindarat, T., Resasco, D. E. & Jongpatiwut, S. Synergistic effect of oxygen vacancies and highly dispersed Pd nanoparticles over Pd-loaded TiO2 prepared by a single-step sol–gel process for deoxygenation of triglycerides. *Appl Catal A Gen* **566**, 74–86 (2018).

31. Pham, V. V. *et al.* Photoreduction route for Cu2O/TiO2 nanotubes junction for enhanced photocatalytic activity. *RSC Adv* **8**, (2018).

32. Wendt, S. *et al.* Oxygen vacancies on TiO2(1 1 0) and their interaction with H2O and O2: A combined high-resolution STM and DFT study. *Surf Sci* **598**, 226–245 (2005).

33. Diebold, U. The surface science of titanium dioxide. *Surf Sci Rep* **48**, 53–229 (2003).

34. Canton, P. *et al.* Pd/CO average chemisorption stoichiometry in highly dispersed supported Pd/γ-Al2O3 catalysts. *Langmuir* **18**, 6530–6535 (2002).

35. Huber, G. W. & Corma, A. Synergies between bio- and oil refineries for the production of fuels from biomass. *Angewandte Chemie - International Edition* vol. 46 Preprint at https://doi.org/10.1002/anie.200604504 (2007).

36. Kerkel, F., Markiewicz, M., Stolte, S., Müller, E. & Kunz, W. The green platform molecule gamma-valerolactone - ecotoxicity, biodegradability, solvent properties, and potential applications. *Green Chemistry* **23**, (2021).

37. Sun, D. *et al.* Production of C4 and C5 alcohols from biomass-derived materials. *Green Chemistry* vol. 18 Preprint at https://doi.org/10.1039/c6gc00377j (2016).

38. Tomishige, K., Nakagawa, Y. & Tamura, M. Design of supported metal catalysts modified with metal oxides for hydrodeoxygenation of biomass-related molecules. *Current Opinion in Green and Sustainable Chemistry* vol. 22 Preprint at https://doi.org/10.1016/j.cogsc.2019.11.003 (2020).

39. Kim, S. *et al.* Recent advances in hydrodeoxygenation of biomass-derived oxygenates over heterogeneous catalysts. *Green Chem.* **21**, 3715–3743 (2019).

40. Gomez, L. A., Bavlnka, C. Q., Zhang, T. E., Resasco, D. E. & Crossley, S. P. Revealing the Mechanistic Details for the Selective Deoxygenation of Carboxylic Acids over Dynamic MoO3 Catalysts. *ACS Catal* **13**, (2023).

41. Gilkey, M. J., Mironenko, A. V., Yang, L., Vlachos, D. G. & Xu, B. Insights into the Ring-Opening of Biomass-Derived Furanics over Carbon-Supported Ruthenium. *ChemSusChem* **9**, 3113–3121 (2016).

42. Attia, S., Schmidt, M. C., Schröder, C. & Schauermann, S. Formation and Stabilization Mechanisms of Enols on Pt through Multiple Hydrogen Bonding. *ACS Catal* **9**, 6882–6889 (2019).